

## Long-Time Phase Correlations Reveal Regulation of Beating Cardiomyocytes

Ohad Cohen<sup>1</sup>, Ido Nitsan,<sup>2</sup> Shelly Tzlil,<sup>2</sup> and Samuel A. Safran<sup>1</sup>

<sup>1</sup>*Department of Chemical and Biological Physics, Weizmann Institute of Science, Rehovot 76100, Israel*

<sup>2</sup>*Faculty of Mechanical Engineering, Technion, Israel Institute of Technology, Haifa 32000, Israel*



(Received 29 June 2020; accepted 6 November 2020; published 18 December 2020)

Spontaneous contractions of cardiomyocytes are driven by calcium oscillations due to the activity of ionic calcium channels and pumps. The beating phase is related to the time-dependent deviation of the oscillations from their average frequency, due to noise and the resulting cellular response. Here, we demonstrate experimentally that, in addition to the short-time (1–2 Hz), beat-to-beat variability, there are long-time correlations (tens of minutes) in the beating phase dynamics of isolated cardiomyocytes. Our theoretical model relates these long-time correlations to cellular regulation that restores the frequency to its average, homeostatic value in response to stochastic perturbations.

DOI: 10.1103/PhysRevLett.125.258101

**Introduction.**—Understanding the beating dynamics of heart cells is important, since its variability may be related to various diseases [1–4]. Recent experiments [5] showed that the beating rate of isolated cardiomyocytes can be entrained by (synchronized to) a nearby mechanical probe via elastic interactions mediated by the surrounding matrix [6]. Surprisingly, it was observed that, while the beating rate was 1–2 Hz, about 15 min elapsed until the cell was entrained. When the probe was stopped, the cell returned to its intrinsic, spontaneous frequency only after about an hour. Since the cells in those experiments are isolated and propagation of the elastic signal is fast [6], the origin of these apparent long timescales must stem from internal biochemistry of the cardiomyocyte.

Motivated by these pacing experiments by Nitsan *et al.* [5], we present here a conceptual hypothesis that relates the apparent long timescales to cardiomyocyte biochemistry, even in the absence of an external probe. Inspired by the “fluctuation-dissipation” response of physical systems, we hypothesized that the long timescales of entrainment originate in the intrinsic dynamical response of the cell to perturbations of its spontaneous oscillation frequency. To validate our hypothesis, we designed and carried out new experiments that measure the beating dynamics of isolated cells over many hours. We analyze those experiments using a simple theory (based on previously derived considerations of calcium channels and pumps activity [7–12]) that considers a competition of biochemical homeostasis and noise. Our combined results demonstrate that, even in the absence of an external probe, deviations of the beating frequency from its average value are characterized by a long timescale of the order of tens of minutes.

Cellular stochasticity results in deviations of the oscillations from their average value. We show theoretically that biological regulation that slowly restores these deviations to their homeostatic value results in long-time phase

correlations. We therefore denote the characteristic time for these correlations as the “regulation time”  $\tau_r$ . Analyzing the long-time phase correlations measured in our experiments, we show that the data for different cells, for times shorter than  $\tau_r$ , collapse onto a theoretically predicted, universal curve for the time-dependent variance of the beating phase. This demonstrates that all the analyzed cells share common dynamics, with a predicted regulation time on the order of many minutes. Our experiments show that the long-time correlations are still observed even when contractility is inhibited by blebbistatin, suggesting that mechanical contraction is not essential for these correlations. Moreover, we observe that inhibiting the activity of  $\text{Ca}^{2+}$ /calmodulin-dependent protein kinase II (CamKII), an enzyme involved in regulation of the RyR channels, results in a much longer regulation time for the beating dynamics. Thus, the value of the regulation time may give insight to the mechanisms related to  $\text{Ca}^{2+}$  channels that regulates spontaneous beating in cardiac cells [13,14].

**Theory.**—Spontaneous calcium oscillations with a single deterministic frequency have been theoretically related to the dynamics of calcium channels and pumps [11,12,15–17], resulting in the simple model presented in Refs. [9,10]. The spontaneous nature of the oscillations is driven by the feedback effect known as “calcium-induced calcium release” (CICR) by which the ion channel activity is modulated by the calcium released through the channel. We previously showed [9,10] that this feedback can be quantified from the measured properties of the RyR channel dynamics and derived a simple, van der Pol–like [18] equation that predicts spontaneous  $\text{Ca}^{2+}$  oscillations when the CICR feedback effect is large enough (derivations briefly reviewed in Supplemental Material [19]):

$$c''(t) + \gamma \dot{c}(t) + \Gamma c(t)^2 \dot{c}(t) + \Omega_c^2 c(t) = 0, \quad (1)$$

where  $c(t)$  is the deviations of calcium concentration from their average. The linear (nonlinear) “friction”  $\gamma$  ( $\Gamma$ ) and deterministic, homeostatic frequency  $\Omega_c$  originate from the *average* activity and CICR feedback of RyR channels and calcium pumps (for a derivation, see Ref. [9]). Here, we focus on stochastic effects on the oscillation frequency. Stochastic effects due to biological noise can be accounted for in two ways: (i) As an additive, kinetic “force”  $\eta(t)$  which is added to the right-hand side of the dynamical equation, Eq. (1) or (2), as stochastic fluctuations in the concentration of signaling molecules, that affect pump and channel activity and, therefore, the frequency. Biological regulation then restores the ion channel and pump activity, from their noisy, stochastic values back to the deterministic frequency  $\Omega_c$ . We show below that the source of the observed, long-time correlations is associated with an effectively noisy oscillation frequency  $\Omega(t)$ , whose average over the noise is  $\langle \Omega(t) \rangle = \Omega_c$ . The additive stochastic force  $\eta(t)$  results in *short-time* fluctuations of the beating frequency about its spontaneous value  $\Omega_c$ , which are commonly referred to as the “beat-to-beat variability.”

In this Letter, we focus on the *long-time* deviations of the instantaneous beating frequency  $\Omega(t)$  [after averaging over  $\eta(t)$ , the short-term noise] from its deterministic, average value of  $\Omega_c$ . Such deviations come from the response of the cell to noise via slow regulation of the beating frequency by the cell through biochemical feedback loops. These occur on a much longer timescale and are related in our model to regulation of the beating frequency by a generic degree of freedom that represents (for example) a change in the RyR channel and Sarco/endoplasmic reticulum  $\text{Ca}^{2+}$ -ATPase pump activity. Any modulation of these activities will change the balance of calcium fluxes, resulting in modulation of the beating frequency. For example, regulation of the frequency may be accomplished by variation of the concentration of phosphorylated RyR channels (the general case is discussed in Supplemental Material [19], with the results qualitatively the same). The concentration may vary stochastically about a steady state, homeostatic value, dictated by cellular conditions. Since the oscillation frequency originates in the RyR channel activity, this gives rise to a stochastic dynamical equation for the time evolution of the frequency  $\Omega(t)$  due to both the noise and the homeostatic regulation:

$$\frac{d\Omega(t)}{dt} = -\frac{1}{\tau_r} [\Omega(t) - \Omega_c] + \xi(t). \quad (2)$$

The noise  $\xi(t)$  is taken to be delta correlated in time on the long timescale:  $\langle \xi(t)\xi(t') \rangle = D\delta(t-t')$ . The frequency, perturbed by the noise, is slowly restored to its homeostatic value by biological regulation, represented by the term  $\sim [\Omega(t) - \Omega_c]/\tau_r$ . In our example, this “homeostatic force” represents a biochemical feedback loop that works to restore the concentration of activated channels, and, hence, the

oscillation frequency to its homeostatic value  $\Omega_c$ , by modulating various signaling pathways not explicitly included here [16,20–22]. In Supplemental Material [19], we give an example of how regulation of a specific property (such as the concentration of activated channels) gives rise to an effective equation for the regulation of the frequency as in Eq. (2). Note that, for a mechanically paced cell, the spontaneous frequency  $\Omega_c$  is replaced by the external pacing frequency, which results in a relaxation to the pacing frequency instead. This is true for any external perturbation that changes the spontaneous beating frequency of the cell. The typical timescale of this regulation is  $\tau_r$ , the “regulation time,” which our experiments show is much longer than the beating frequency, as explained below.

With the inclusion of noise and regulation of the frequency  $\Omega(t)$ , we have two coupled equations for the instantaneous calcium concentration [Eq. (1)] and the effective dynamics of the frequency [Eq. (2)]. Defining the deviations of the frequency from its average  $\Delta\Omega(t) = \Omega(t) - \Omega_c$ , the solution of Eq. (2) results in an expression for time decay of the correlations  $\Delta\Omega$ , characterized by the homeostatic regulation time  $\tau_r$ :

$$C(t-t') = \langle \Delta\Omega(t)\Delta\Omega(t') \rangle = D\tau_r e^{-|t-t'|/\tau_r}. \quad (3)$$

With mean square frequency deviations,

$$\langle [\Delta\Omega(t) - \Delta\Omega(t')]^2 \rangle = 2D\tau_r(1 - e^{-|t-t'|/\tau_r}). \quad (4)$$

From Eq. (4), we see that the mean square deviations of the frequency grow linearly in time for times shorter than the regulation time ( $|t-t'| \ll \tau_r$ ) and saturate at a constant value of  $2\sigma^2 = 2D\tau_r$  for long times  $|t-t'| \gg \tau_r$ , where  $\sigma$  is the standard deviation of the distribution of  $\Delta\Omega$ . Thus, the larger  $\tau_r$ , the longer the time over which the frequency “diffuses” before frequency deviations are saturated. When translated to the homeostatic force that restores the frequency to its average value, large  $\tau_r$  corresponds to a weak homeostatic restoring force [see Eq. (2)], while small values of  $\tau_r$  correspond to strong homeostatic force.

On short times, the fluctuations in frequency (relative to its average) translate to a delay or an advance between consecutive beats. These deviations not only affect the local dynamics, but also accumulate so that, over time, several beats are skipped or added compared to regular beating with the fixed frequency  $\Omega_c$ . This accumulation can be expressed in terms of the time-dependent beating phase, defined for the calcium concentration as an integral over the time-dependent frequency (see [23] and Supplemental Material [19] for a derivation):

$$c(t) = c\left(\int \Omega(t)dt\right) = c[\Omega_c t + \phi(t)], \quad (5)$$

where a constant phase is equivalent to  $\Delta\Omega = 0$  and the phase dynamics obeys  $d\phi/dt = \Delta\Omega$ . Using the definition

of Eq. (5) and the result of Eq. (3), we calculate the mean square difference of the phase at two times, i.e., the temporal phase variance  $\delta\phi^2(t-t') = \langle [\phi(t) - \phi(t')]^2 \rangle$  (see Sec. D in Supplemental Material [19]):

$$\delta\phi^2(t-t') = 2D\tau_r^3 \left( \frac{|t-t'|}{\tau_r} - 1 + e^{-|t-t'|/\tau_r} \right). \quad (6)$$

If the time interval  $\tau = |t-t'|$  is short compared to the regulation time ( $\tau \ll \tau_r$ ), the phase variance grows quadratically in time  $\sim \tau^2$ . This is because  $\delta\phi^2$  is a temporal integral of the frequency variance, which at short times grows linearly with  $\tau$ . If the time interval is long compared to the regulation time ( $\tau \gg \tau_r$ ), the phase variance grows linearly in time. This is because at long times the regulation of the frequency comes into effect, which yields a constant frequency variance. Therefore, the profile of decay of correlations in frequency ( $\sim \dot{\phi}$ ) and the subsequent time dependence of the phase variance quantifies the intrinsic timescales due to noise and homeostasis in the system. The theoretical predictions for the  $\delta\phi^2$  motivated long-time experimental measurements. Below, we show that analyzing the experiments in terms of the phase variance allows us to extract the regulation time  $\tau_r$  and results in a collapse of the data for different cells with different values of  $\tau_r$  onto a universal curve predicted by Eq. (6).

*Experiment.*—Neonatal rat cardiomyocytes were cultured on a micropatterned, elastic substrate, embedded with fluorescent beads (see methods in Sec. A in Supplemental Material [19], which includes Refs. [24–26]). The cultured cells beat spontaneously, generating significant substrate deformations along the contraction axis (long axis of the cell), which results in an oscillatory, stochastic signal representing the contraction-relaxation cycle (see Fig. S7 in Sec. G in Supplemental Material [19]).

Each cell was monitored continuously for 2 min (henceforth referred to as “short experiments”), in order to ascertain that the beating was relatively stable. The instantaneous and average frequencies were then estimated using wavelet analysis. For each cell, the beating dynamics was then tracked in fixed intervals of 1–2.5 min, where in each interval the cell was imaged continuously for  $\sim 7.7$ –15 s, for a total duration of  $\sim 4$ –10 h (henceforth referred to as “long experiments”). The average frequency in each interval was then estimated from the inverse of the average peak-to-peak time (see Sec. E in Supplemental Material [19]). This method effectively averages out the short-term noise, allowing us to focus on the long-term stochastic effects [due to  $\xi(t)$ ], and yields a coarse-grained, average frequency  $\Omega_c(t) = 0.87 \pm 0.34$  Hz ( $n = 16$ ).

In both the short and long experiments, we measure the deviation of the frequency from its average via the frequency difference  $\Delta\Omega(t) = (\Omega_c(t) - \langle \Omega_c \rangle)$ . For the short experiments,  $\Delta\Omega$  is the difference between the instantaneous frequency and its average (evaluated over 2 min).

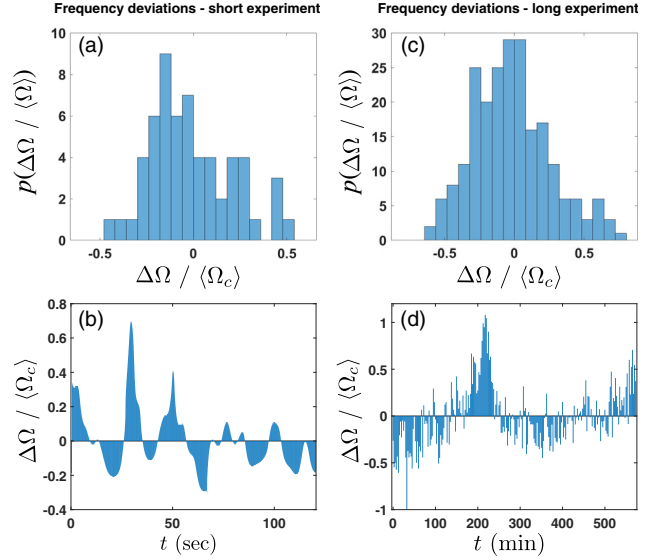


FIG. 1. The distribution (a),(c) and time evolution (b),(d) of the beating frequencies normalized by the average beating frequency for a representative cell. For the short experiments (left), the beating was tracked continuously for 2 min (a),(b), and the frequencies were evaluated using wavelet analysis and are normalized by the 2 min average frequency. For the long experiments, the beating was tracked intermittently for  $\sim 7.7$ –15 s at intervals of 1–2.5 min (c),(d). The frequency within each interval is calculated as the average of the inverse peak-to-peak time (which yields similar results when calculated by wavelet analysis; see Sec. E in Supplemental Material [19]) and is normalized by the average frequency of the entire experiment (4–10 h).

For the long experiments,  $\Delta\Omega$  is the difference between the coarse-grained frequency of each interval and its average over the entire experiment (evaluated over  $\sim 4$ –10 h).

Figure 1 compares the distribution of  $\Delta\Omega$  for the short and long experiments [Figs. 1(a) and 1(c)], as well as their evolution in time [Figs. 1(b) and 1(d)], for a representative cell. The frequency fluctuations over time were similar in both cases, with an average standard deviation  $\sigma = 0.192 \pm 0.171$  Hz and  $\sigma = 0.157 \pm 0.091$  Hz ( $n = 16$ ) for the short and long experiments, respectively. However, while for the short experiments the instantaneous frequency remains correlated over several seconds, for the long experiments the coarse-grained frequency remains correlated over many minutes [see Figs. 1(b) and 1(d) and Sec. D in Supplemental Material [19]]. Our focus is only on the long-term noise, for which the frequency fluctuations are related to the model parameters via  $\sigma^2 = D\tau_r$ .

As explained in the previous section, the beating phase is defined as the temporal integral of the frequency difference  $\Delta\Omega$  for the long experiments (where the contribution due to the short-term noise is averaged out by our coarse-graining method). Note that, in order to obtain the phase for the long experiments, we interpolated the value of the coarse-grained frequency  $\Omega_c(t)$  in each interval to vary linearly

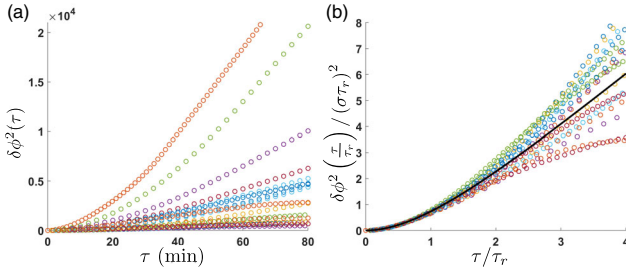


FIG. 2. (a) Temporal phase variance  $\delta\phi^2(\tau)$  as measured for the different cells in the long experiments, plotted as a function of time  $\tau$ , and (b) the same variance scaled to the frequency variance ( $\sigma^2$ ) and plotted as a function of the scaled time  $\tau/\tau_r$ . Here  $\sigma^2$  is evaluated from the width of the distribution of frequencies, and  $\tau_r$  is estimated from the linearization of the temporal variance scaled by  $\tau^2$ . The scaled version of the analytical result of Eq. (6) is also plotted (black line).

between intervals. In Fig. 2(a), we plot the experimental equivalent of  $\delta\phi^2(\tau)$ , as a function of the time lag  $\tau = |t - t'|$ . Consistent with our derivation in Eq. (6),  $\delta\phi^2(\tau)$  shows a quadratic increase at short times and a linear increase in longer times (see Fig. 2 and Fig. S2 in Supplemental Material [19]). This suggests a transition from a regime where regulation of the frequency is in progress (the frequency variance increases linearly with time) to a long-time regime ( $t \gg \tau_r$ ) where the frequency reaches its homeostatic value (the frequency variance saturates at a constant value).

To show that indeed all cells follow similar dynamics, we evaluate  $\tau_r$  from a linearization of  $\delta\phi^2(\tau)/\tau^2$  (see Sec. D in Supplemental Material [19] for details), which results in an average regulation time  $\tau_r = 17.9 \pm 7.2$  min ( $n = 16$ ). We use this estimate of  $\tau_r$ , along with the previously calculated frequency variance  $\sigma^2$ , to plot the scaled version of the phase variance  $\sim \delta\phi^2(T)/(\sigma\tau_r)^2$ , where we define the scaled time  $T = \tau/\tau_r$ . Figure 2(b) shows the dimensionless, rescaled variance as a function of rescaled time for all cells. One can see that, up until the regulation time (of the order of  $\sim 10$  min), the data collapse on a curve given by the similarly scaled version of Eq. (6) (black line), validating our theory. At longer times, deviations from the theory occur, possibly due to another regulatory process with additional timescales, which require an extension of our theory (see Sec. F in Supplemental Material [19] for one possible extension).

**Biochemical perturbations.**—In a separate set of experiments, we culture the cells with  $2.5 \mu\text{M}$  of blebbistatin, which inhibits myosin activity and, hence, actomyosin contractility. As evidenced in Sec. G in Supplemental Material [19], long-time regulation of the average beating frequency still persists even when contractility is inhibited. Therefore, actomyosin activity is not essential for long-time regulation of beating.

To obtain insight into the processes that control regulation and the value of  $\tau_r$ , we conducted a separate set of

experiments, where cells were cultured with  $10 \mu\text{M}$  auto-camtide-2-related inhibitory peptide (AIP), which inhibits  $\text{Ca}^{2+}$ /calmodulin-dependent protein kinase II (CaMKII) activity that is known to regulate RyR kinetics [27,28]. The beating dynamics of each cell were measured for  $\sim 4$  h, then AIP was applied, and the dynamics were measured for an additional  $\sim 6$  h. We then calculated and compared for each cell the average beating frequency and regulation time before and after culturing with AIP (see Sec. G in Supplemental Material [19]). Interestingly, we find that across all cells ( $n = 7$ ) the regulation time  $\tau_r$  increase considerably when AIP is introduced. For these experiments, the regulation time with AIP was increased by an average factor of  $\sim 2.5$  ( $\tau_r/\tau_0 = 2.55 \pm 0.30$ , where the subscript 0 denotes the measurement before AIP application). The strong dependence of the value of  $\tau_r$  on CaMKII activity suggests that biochemical modification of channels and enzymes that regulate calcium dynamics plays a major role in the feedback loop that drives the cell back to homeostasis after perturbation by noise. The changes in the regulation time due to AIP suggests that this biochemical modification slows the homeostatic response that restores the beating frequency to its average.

**Discussion.**—At the organ level, it was shown that long-time correlations in the beating rate, or lack thereof, are associated with certain pathological conditions [29,30]. Our single-cell experiments and theory show that such long-time correlations are apparent even at the single-cell level and do not necessarily involve intercellular interaction. We show that, while correlations between consecutive beats decay over short times (seconds), there are significant long-time correlations (minutes) in the beating dynamics of isolated cardiomyocytes due to slow modulations of the frequency. These correlations are characterized by a regulation time  $\tau_r \sim 20$  min, much longer than the timescales associated with beating ( $\sim 1$  s). The long regulation time may originate from slow, coupled biochemical feedback loops that drive cell back to homeostasis. Our mean field theory considers the “average” channel and pump dynamics and suggests that regulation of these can affect the instantaneous oscillation frequency [16,20,22].

We further show that inhibiting contractility with blebbistatin did not diminish the long-time correlations in cultured cells. This implies that electromechanical coupling is not necessary for long-time correlations, although it can obviously modulate them. Additionally, we have shown that culturing cells with AIP (that inhibits CaMKII activity) results in an increase in the regulation time, probably by interfering with regulation of calcium dynamics.

Recent experiments and theory have shown that mechanical pacing of isolated cells (by a nearby cell or an inert mechanical probe) can significantly reduce the short-term fluctuations (beat-to-beat variability) in amplitude and frequency after  $\sim 10$ – $15$  minutes of “training” [31,32]. Additionally, cells synchronized to an oscillating mechanical probe within  $10$ – $15$  min and maintain beating with the

spacing frequency for 1 h after the pacing has stopped. These timescales for mechanical communication between cells are comparable to the observed regulation time [5]. It was further shown that mechanical noise reduction involves enzymatic activity (e.g., CaMKII). The similarity between the timescale for mechanical communication and the value of  $\tau_r$  and the involvement of CaMKII both in mechanical communication and in modulating the “regulation time” suggests that the same regulation mechanism which controls the recovery of a cell from stochastic perturbations is responsible for the slow kinetics of mechanical communications. It will also be interesting to see how the observed regulation time varies for a multicell cluster or assembly of interacting cardiomyocytes [33], which may indicate the role of  $\tau_r$  in tissue analogs.

The ability to maintain and regulate coherent beating is crucial for the viability of beating cardiomyocytes. The regulation time as well as the temporal variance of the beating are simple, noninvasive metrics that can serve as indicators for possible cardiomyocyte dysfunction.

The authors thank A. Grosberg, S. Drori, D. Deviri, S. K. Nandi, K. Dasbiswas, and R. Adar for useful discussions. S. A. S. is grateful to the Kretner-Katz and Perlman family foundations for support.

- 
- [1] E. J. Benjamin, S. S. Virani, C. W. Callaway, A. M. Chamberlain, A. R. Chang, S. Cheng, S. E. Chiuve, M. Cushman, F. N. Dellings, R. Deo *et al.*, *Circulation* **137**, e67 (2018).
- [2] M. A. Gatzoulis, S. Balaji, S. A. Webber, S. C. Siu, J. S. Hokanson, C. Poile, M. Rosenthal, M. Nakazawa, J. H. Moller, P. C. Gillette *et al.*, *Lancet* **356**, 975 (2000).
- [3] J. F. Thayer, S. S. Yamamoto, and J. F. Brosschot, *International Journal of Cardiology* **141**, 122 (2010).
- [4] H. Tsuji, F. J. Venditti, Jr., E. S. Manders, J. C. Evans, M. G. Larson, C. L. Feldman, and D. Levy, *Circulation* **90**, 878 (1994).
- [5] I. Nitsan, S. Drori, Y. E. Lewis, S. Cohen, and S. Tzlil, *Nat. Phys.* **12**, 472 (2016).
- [6] O. Cohen and S. A. Safran, *Soft Matter* **12**, 6088 (2016).
- [7] D. M. Bers, *Nature (London)* **415**, 198 (2002).
- [8] S. Sirenko, V. A. Maltsev, L. A. Maltseva, D. Yang, Y. Lukyanenko, T. M. Vinogradova, L. R. Jones, and E. G. Lakatta, *J. Mol. Cell. Cardiol.* **66**, 106 (2014).
- [9] O. Cohen and S. A. Safran, *Phys. Rev. Lett.* **122**, 198101 (2019).
- [10] O. Cohen and S. A. Safran, *Frontiers of oral physiology* **11**, 164 (2020).
- [11] J. Sneyd, J. M. Han, L. Wang, J. Chen, X. Yang, A. Tanimura, M. J. Sanderson, V. Kirk, and D. I. Yule, *Proc. Natl. Acad. Sci. U.S.A.* **114**, 1456 (2017).
- [12] S. Galice, Y. Xie, Y. Yang, D. Sato, and D. M. Bers, *J. Am. Heart Assoc.* **7**, e008724 (2018).
- [13] S. Hu, K. Dasbiswas, Z. Guo, Y.-H. Tee, V. Thiagarajan, P. Hersen, T.-L. Chew, S. A. Safran, R. Zaidel-Bar, and A. D. Bershadsky, *Nat. Cell Biol.* **19**, 133 (2017).
- [14] A. J. Engler, C. Carag-Krieger, C. P. Johnson, M. Raab, H.-Y. Tang, D. W. Speicher, J. W. Sanger, J. M. Sanger, and D. E. Discher, *J. Cell Sci.* **121**, 3794 (2008).
- [15] G. Dupont, M. Berridge, and A. Goldbeter, *Cell Calcium* **12**, 73 (1991).
- [16] H. H. Valdivia, J. H. Kaplan, G. Ellis-Davies, and W. J. Lederer, *Science* **267**, 1997 (1995).
- [17] E. G. Lakatta, V. A. Maltsev, and T. M. Vinogradova, *Circ. Res.* **106**, 659 (2010).
- [18] J. C. Sprott, *Elegant Chaos: Algebraically Simple Chaotic Flows* (World Scientific, Singapore, 2010).
- [19] See Supplemental Material at <http://link.aps.org/supplemental/10.1103/PhysRevLett.125.258101> for a review of the experimental methods, derivation of the theory, examples of phase and frequency correlations, examples of the fitting procedure and experimental data of AIP and blebbistatin experiments.
- [20] H.-T. Yang, D. Tweedie, S. Wang, A. Guia, T. Vinogradova, K. Bogdanov, P. D. Allen, M. D. Stern, E. G. Lakatta, and K. R. Boheler, *Proc. Natl. Acad. Sci. U.S.A.* **99**, 9225 (2002).
- [21] M. J. Bround, P. Asghari, R. B. Wambolt, L. Bohunek, C. Smits, M. Philit, T. J. Kieffer, E. G. Lakatta, K. R. Boheler, E. D. Moore *et al.*, *Cardiovasc. Res.* **96**, 372 (2012).
- [22] D. M. Bers and E. Grandi, *J. Cardiovasc. Pharmacol.* **54**, 180 (2009).
- [23] P. Hanggi and P. Riseborough, *Am. J. Phys.* **51**, 347 (1983).
- [24] X. Tang, M. Y. Ali, and M. T. A. Saif, *Soft Matter* **8**, 7197 (2012).
- [25] E. Jones, MATLAB based DIC code, The MathWorks Inc., Natick, MA, <http://www.mathworks.com/matlabcentral/fileexchange/43073-improved-digital-image-correlation-dic> (2013).
- [26] E. Jones, M. Silberstein, S. R. White, and N. R. Sottos, *Exp. Mech.* **54**, 971 (2014).
- [27] S. Currie and G. L. Smith, *FEBS Lett.* **459**, 244 (1999).
- [28] E. Picht, J. DeSantiago, S. Huke, M. A. Kaetzel, J. R. Dedman, and D. M. Bers, *J. Mol. Cell. Cardiol.* **42**, 196 (2007).
- [29] C.-K. Peng, J. Mietus, J. M. Hausdorff, S. Havlin, H. E. Stanley, and A. L. Goldberger, *Phys. Rev. Lett.* **70**, 1343 (1993).
- [30] N. Iyengar, C. Peng, R. Morin, A. L. Goldberger, and L. A. Lipsitz, *Am. J. Physiol.* **271**, R1078 (1996).
- [31] O. Cohen and S. A. Safran, *Sci. Rep.* **8**, 2237 (2018).
- [32] H. Viner, I. Nitsan, L. Sapir, S. Drori, and S. Tzlil, *iScience* **14**, 58 (2019).
- [33] A. Grosberg, P. W. Alford, M. L. McCain, and K. K. Parker, *Lab-on-a-Chip* **11**, 4165 (2011).